7. *FURTHER INSIGHTS FROM GRAPH THEORY*

*The interaction analysis conducted in Chapter 6 showed that the interaction measures selected from the literature do not give the full picture of interaction in the case study process. The measures produced different results and gave conflicting recommendations. The common factor in the measures examined was their reliance on the system transfer function matrix **G** which relates the overall inputs and outputs, and hence does not take into account the underlying relationships between these variables. In this Chapter, two approaches based on Graph Theory with the potential to reveal the underlying relationships are investigated.*

7.1 AN APPROACH TO CLOSED LOOP DESIGN USING GRAPH THEORY

It is well known that analysing a system with control loops included will result in a more complete picture of the interaction in the final system. However, closing the control loops will itself add a substantial number of extra loops, which will differ depending on the pairing chosen. This will also increase substantially the computational effort required in any analysis, and will also require tuning the controllers. An approach to closed loop design is explored here initially through a simple example and then to evaluate whether, in the case of the refrigeration system, the outcome can justify the extra effort needed.

7.1.1. A Simple 2 × 2 Example

The proposed closed control loop design approach is presented here through its application to a simple 2 × 2 example. The system considered is defined as:

$$A = \begin{bmatrix} -1 & 1 \\ 1 & -2 \end{bmatrix} \; , \; B = \begin{bmatrix} 2 & -1 \\ 1 & 2 \end{bmatrix} \; , \; C = \begin{bmatrix} 1 & 0 \\ 0 & 1 \end{bmatrix} \; , \; D = \begin{bmatrix} 0 & 0 \\ 0 & 0 \end{bmatrix} \quad (7.1)$$

where **A**, **B**, **C** and **D** are the system matrices defined in Equations 2.1 and 2.2.

Here, the measured variables are also the state variables, hence the matrix **C** is the identity matrix. Therefore, the measured variables are denoted by **x** instead of **y** hereafter.

At steady state, the system matrix **G**(0) is evaluated as:

$$\mathbf{G}(0) = \begin{bmatrix} 5 & 0 \\ 3 & 1 \end{bmatrix} \quad (7.2)$$

And the relative gain array Λ for the system is evaluated as

$$\Lambda = \begin{bmatrix} 1 & 0 \\ 0 & 1 \end{bmatrix} \quad (7.3)$$

which suggests that pairing x_1 with u_1 and x_2 with u_2 will show no interaction.

The steady state signal flow graph (SFG) between the measured variables (here the state variables) of the open loop system is given in Figure 7.1a. Using the full state space model, the SFG identifies the existence of one loop between x_1 and x_2 that represents interaction. Figure 7.1b, using the system transfer function matrix to draw a SFG for inputs and outputs, fails to show the existence of any underlying loops, and thus the internal interaction is hidden. This illustrates clearly that the matrix **G** is not sufficient in analysing interaction as it fails to identify the interacting loops.

Figures 7.1c and 7.1d show the equivalent situations under the two alternative closed loop control pairings. For example, closing x_1-u_1 and x_2-u_2 loops results in five new additional loops in Figure 7.1c, but only three in Figure 7.1d.
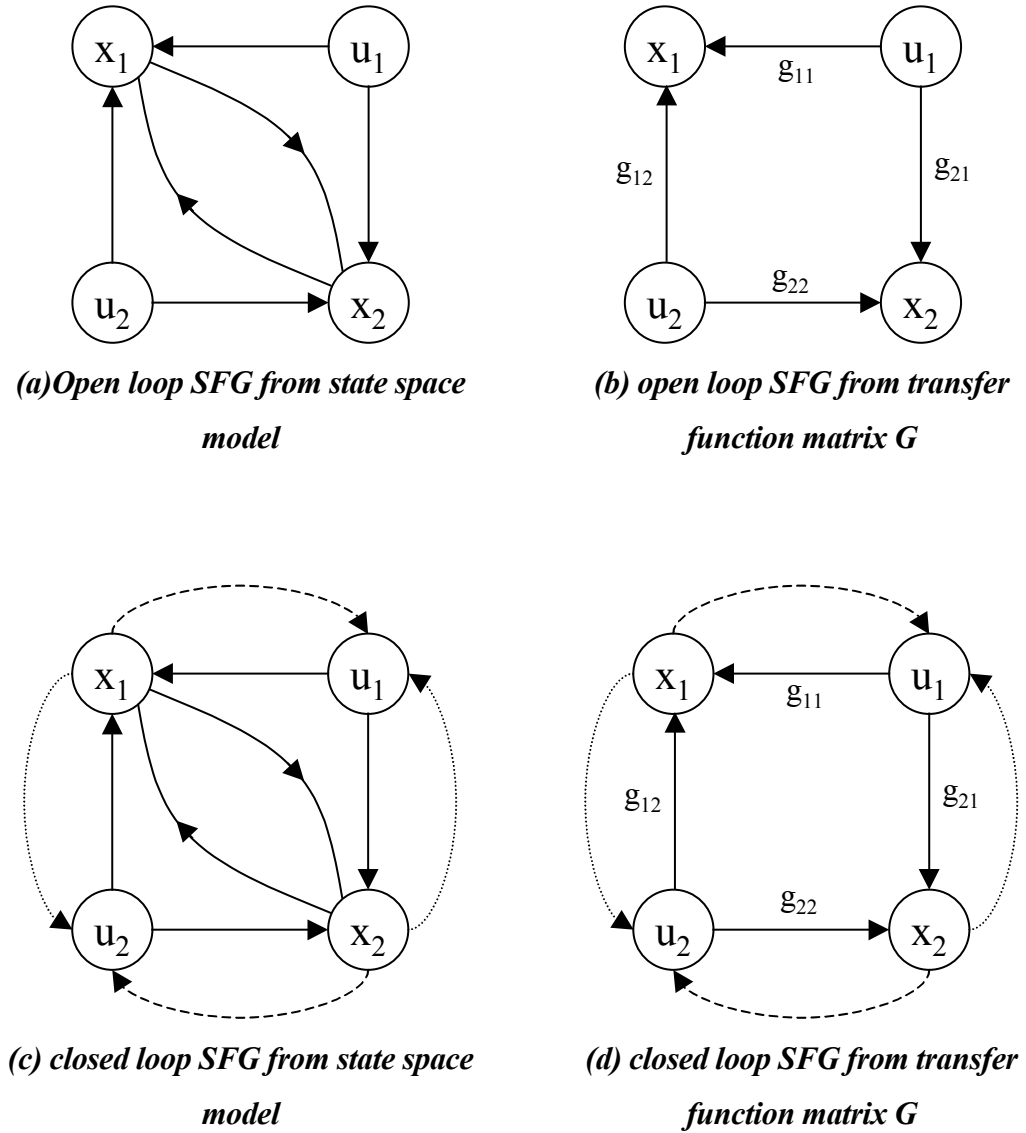

(a)Open loop SFG from state space model

(b) open loop SFG from transfer function matrix G

(c) closed loop SFG from state space model

(d) closed loop SFG from transfer function matrix G

Figure 7.1: Steady state SGF for the 2 $\times$ 2 system defined in Equation 7.1
(---- x_1-u_1 & x_2-u_2 pairing; ⋯⋯ x_1-u_2 & x_2-u_1 pairing)

Extending the analysis into the s-domain, the SFG for the system with the pairing x_1-u_1 and x_2-u_2 is shown in Figure 7.2.
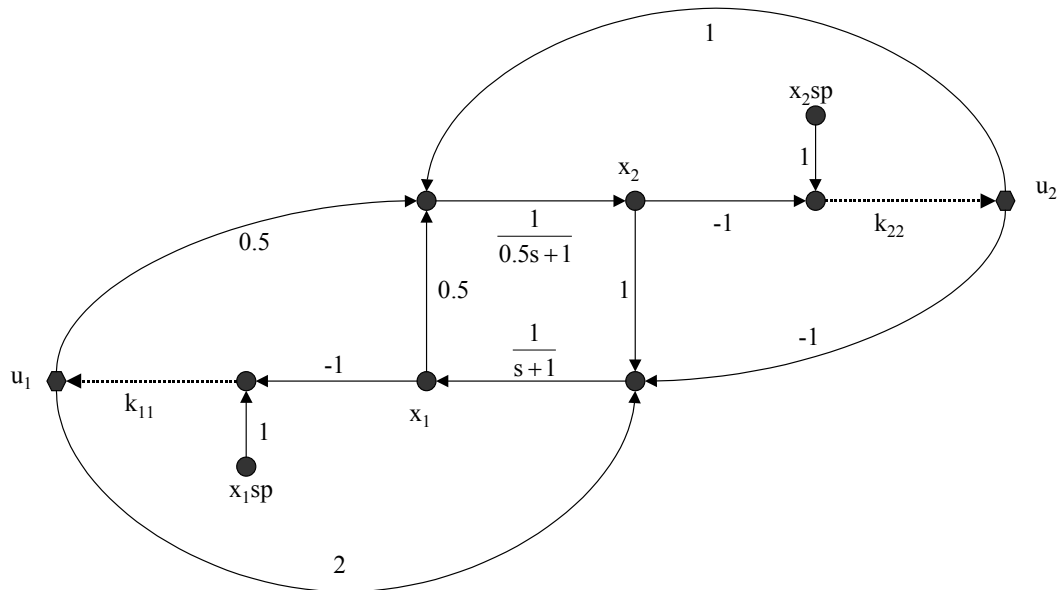
Figure 7.2: SGF for the 2 × 2 system – transfer function representation for the

pairing x₁-u₁ & x₂-u₂

(proportional controllers are shown as ⁗)

The two input / output open loop transfer functions (i.e. $k_{11} = k_{22} = 0$) in Figure 7.2 reduce to:

$$\frac{x_1(s)}{u_1(s)} = \frac{(2)\dfrac{1}{s+1}+(0.5)\dfrac{1}{0.5s+1}(1)\dfrac{1}{s+1}}{1-[0.5\dfrac{1}{0.5s+1}(1)\dfrac{1}{s+1}]} = \frac{s+5}{s^2+3s+1} \tag{7.4}$$

and

$$\frac{x_2(s)}{u_2(s)} = \frac{(1)\dfrac{1}{0.5s+1}+(-1)\dfrac{1}{s+1}(0.5)\dfrac{1}{0.5s+1}}{1-[0.5\dfrac{1}{0.5s+1}(1)\dfrac{1}{s+1}]} = \frac{2s+1}{s^2+3s+1} \tag{7.5}$$

The change in the stability of the control system for change in the gain values k_{11} and k_{22} is an indicator of the interaction caused by one loop on the other loops in the

system. The Routh Stability Criterion and the Routhian Array can be used to determine stability conditions for the system.

Using the Routhian Array to examine the stability of the individual SISO control loops in the system results in the following limits

$$k_{11} \geq -0.2 \tag{7.6a}$$
$$k_{22} \geq -1.0 \tag{7.6b}$$

Closed loop transfer functions can be determined from the SFG in Figure 7.2 by the application of Mason's Rule (Henley and Williams, 1973; D'Azzo and Houpis, 1995). In this case, the two closed loop transfer functions can be obtained as:

$$\frac{x_1(s)}{u_1(s)} = \frac{(2)\frac{1}{s+1}[1-(1)\frac{1}{0.5s+1}(-1)(k_{22})] + (0.5)\frac{1}{0.5s+1}(1)\frac{1}{s+1} + (0.5)\frac{1}{0.5s+1}(-1)(k_{22})(-1)\frac{1}{s+1}}{1 - [(1)\frac{1}{0.5s+1}(-1)(k_{22}) + 0.5\frac{1}{0.5s+1}(1)\frac{1}{s+1} + 0.5\frac{1}{0.5s+1}(-1)(k_{22})(-1)\frac{1}{s+1}]} \tag{7.7}$$

which reduces to

$$\frac{x_1(s)}{u_1(s)} = \frac{s + 2.5k_{22} + 2.5}{0.5s^2 + (1.5 + k_{22})s + (0.5 + 0.5k_{22})} \tag{7.8}$$

and

$$\frac{x_2(s)}{u_2(s)} = \frac{(1)\frac{1}{0.5s+1}[1-(2)\frac{1}{s+1}(-1)(k_{11})] + (-1)\frac{1}{s+1}(0.5)\frac{1}{0.5s+1} + (-1)\frac{1}{s+1}(-1)(k_{11})(0.5)\frac{1}{0.5s+1}}{1 - [(2)\frac{1}{s+1}(-1)(k_{11}) + (0.5)\frac{1}{0.5s+1}(1)\frac{1}{s+1} + (-1)\frac{1}{s+1}(-1)(k_{11})(0.5)\frac{1}{0.5s+1}]} \tag{7.9}$$

which reduces to

$$\frac{x_2(s)}{u_2(s)} = \frac{s + 2.5k_{11} + 0.5}{0.5s^2 + (1.5 + k_{11})s + (0.5 + 2.5k_{11})} \tag{7.10}$$

The resulting characteristic equation is:

$$0.5s^2 + (1.5 + k_{11} + k_{22})s + (0.5 + 2.5k_{11} + 0.5k_{22} + 2.5k_{11}.k_{22}) = 0 \qquad (7.11)$$

Using the Routhian Array to examine its stability results in the following limits:

$$(k_{11} \geq -0.2 \ \& \ k_{22} \geq -1) \quad \text{or} \quad (k_{11} \leq -0.2 \ \& \ k_{22} \leq -1) \qquad (7.12a)$$

and

$$k_{11} \geq -1.5 - k_{22} \qquad (7.12b)$$

The significance of Equation 7.12 is shown in Figure 7.3. The graph axes are the gain factors of the two controllers. Two distinct regions can be determined; a stable region, and an unstable region. These regions are bounded by the Equations 7.12a and 7.12b respectively.
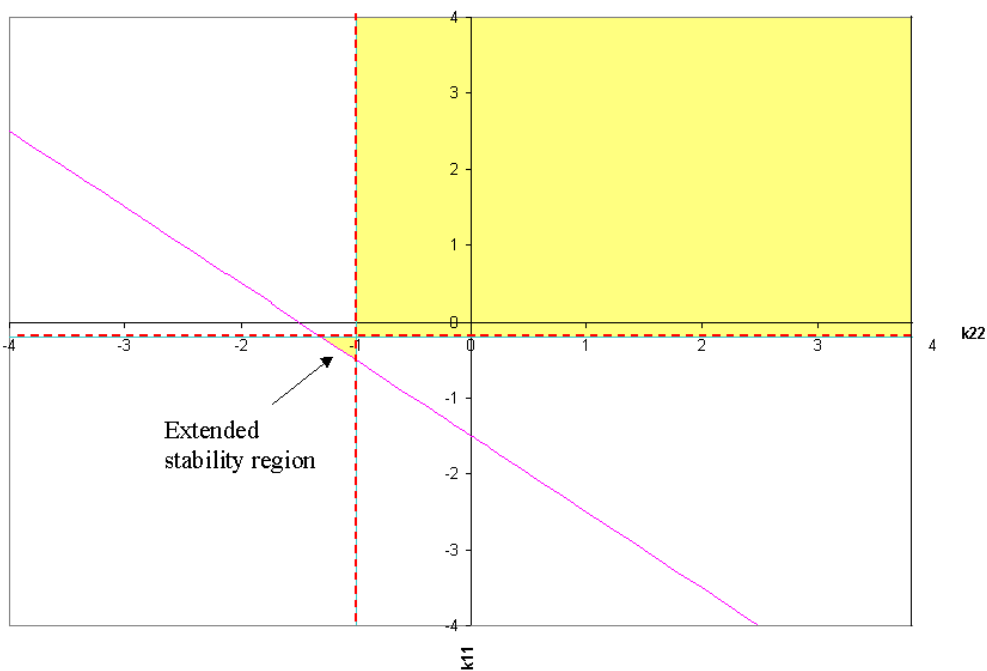

Figure 7.3: Stability of closed loop system for the pairing x_1-u_1 & x_2-u_2 when both loops are closed - yellow areas indicate stable regions

Comparing the stability limits determined from Equation 7.6 for the individual SISO

loops with the stability regions in Figure 7.3 illustrates clearly the effect of interaction between loops in this system, as the presence of both the controllers changes the stability limit of the two separate controllers. It should be noted however that the effect is not always bad, as one controller can extend the range of stability of the other. In Figure 7.3, referring to the x_1-u_1 and x_2-u_2 pairing, the stability region includes a small triangle for $k_{22} < -1$ and $k_{11} < -0.2$. If in this region either of the two controllers is switched to manual, the system will become unstable, however with both control loops closed, the system is stable. Simulation results shown in Figure 7.4 confirm this finding. The two controllers used are proportional controllers with gain factors of -0.25 and -1.1 for k_{11} and k_{22} respectively.
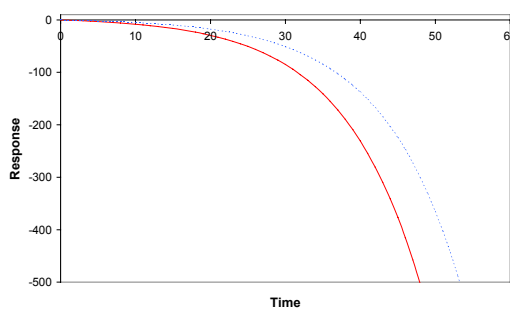
(a) Response to a unit step change in $x_1$sp
(loop x_1-u_1 only on automatic)
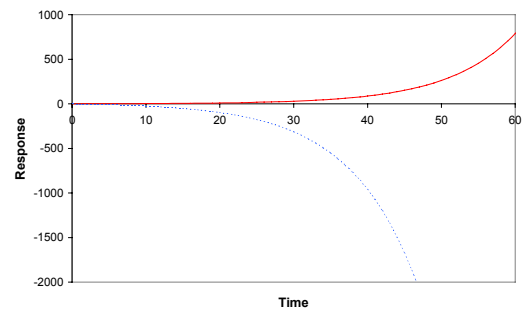
(b) Response to a unit step change in $x_2$sp
(loop x_2-u_2 only on automatic)
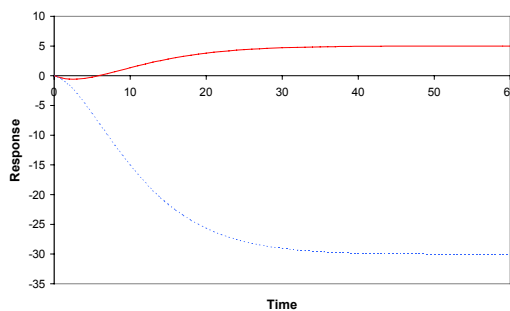
(c) Response to a unit step change in $x_1$sp
(both loops on automatic)
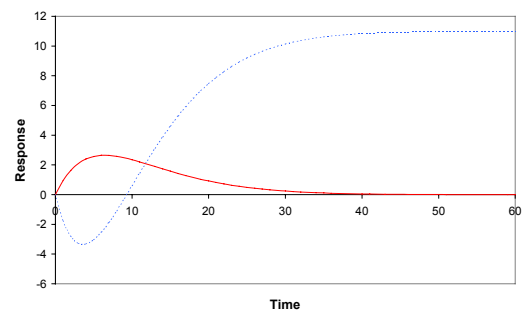
(d) Response to a unit step change in $x_2$sp
(both loops on automatic)

—— x_1 ---- x_2

Figure 7.4: Responses of x_1 and x_2 to unit changes in their set points (x_1-u_1 & x_2-u_2 pairings). Interaction between the loops ensures stability so long as both loops are closed

Similarly, the same analysis was also conducted on the pairing x_1-u_2 and x_2-u_1 shown in Figure 7.5. The resulting characteristic equation is:

$$0.5s^2 + (1.5 + 0.5k_{21} - 0.5k_{12})s + (0.5 + 1.5k_{21} - 2.5k_{12}.k_{21}) = 0 \qquad (7.13)$$
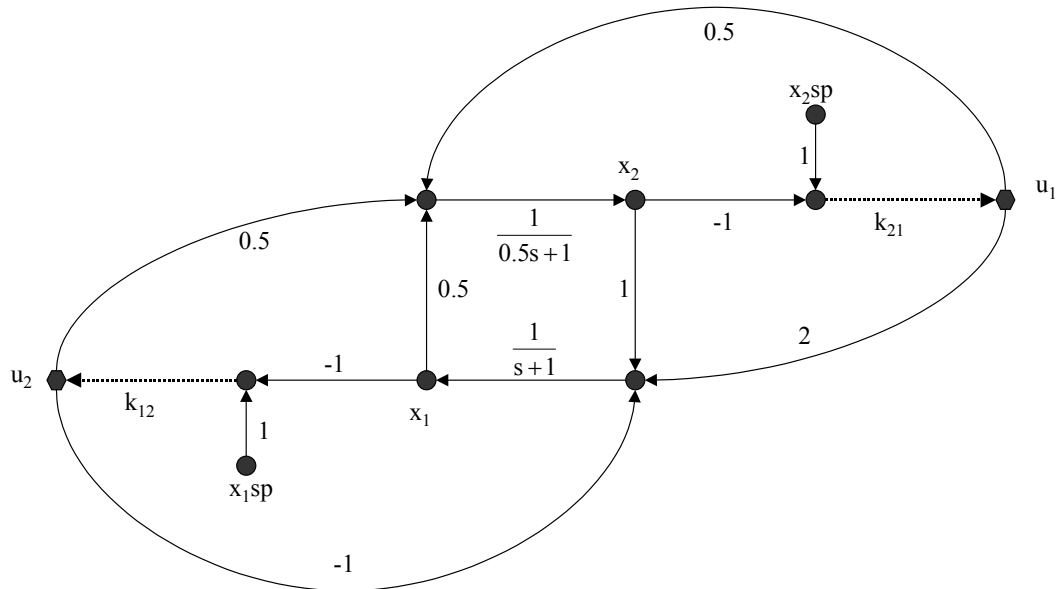
Figure 7.5: SGF for the 2 × 2 system – transfer function representation for the pairing x_1-u_2 & x_2-u_1
(proportional controllers are shown as ····)

Using the Routhian Array, the stability limits for the two input / output loop transfer functions (i.e. $k_{12} = k_{21} = 0$) is:

$$k_{12} \leq 3.0 \qquad (7.14a)$$
$$k_{21} \geq -0.333 \qquad (7.14b)$$

Closing the two loops results in the following stability limits:

$$k_{21} \geq k_{12}\text{-}3 \qquad (7.15a)$$

and

$$k_{21} \geq \frac{1}{5k_{12} - 3} \qquad (7.15b)$$

Figure 7.6 shows the stability regions for the alternative pairings x_1-u_2 and x_2-u_1 determined by Equations 7.15a and 7.15b. Examining this graph shows two important features:

1. The stability region expands to include a small triangular area when k_{12} is greater than 3, and also a large area when k_{21} is smaller than –0.333. This behaviour has also been seen in Figure 7.3.

2. The area of stability of the system was reduced in other areas in Figure 7.6, which are bounded by Equation 7.15b. For example if k_{21} and k_{12} were set to 1, each loop is stable on its own, but placing both loops on automatic results in an unstable system. This is confirmed by simulation in Figure 7.7.
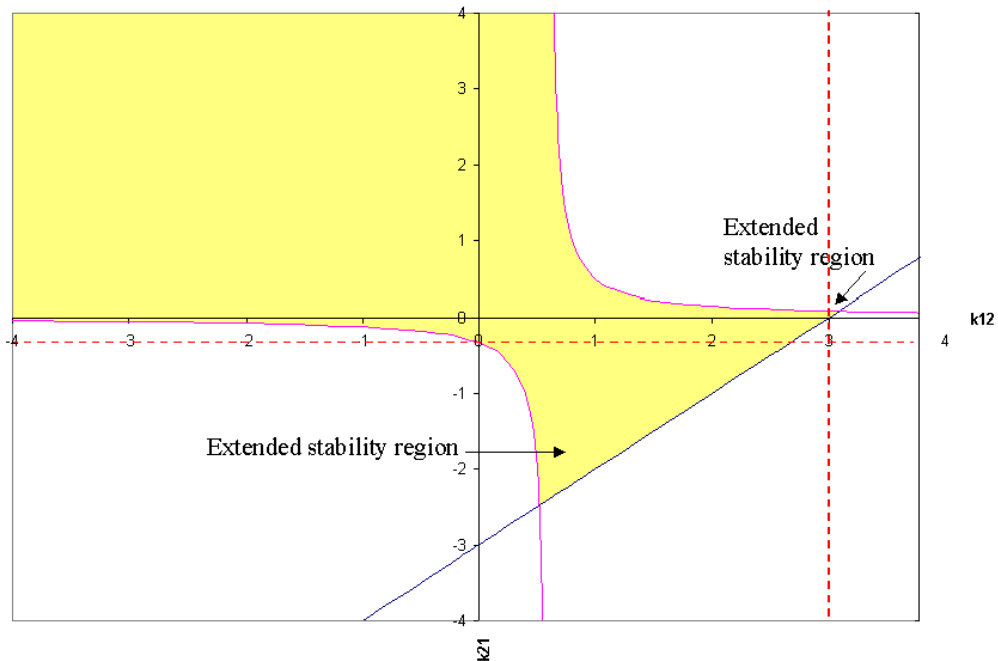
Figure 7.6: Stability of closed loop system for the pairings x_1-u_2 & x_2-u_1 when both loops are closed - yellow areas indicate stable regions

The two cases examined in analysing this simple example illustrate clearly that graphs similar to Figures 7.3 and 7.6 can be used as a design tool in visualising regions of stability in systems of multiple SISO control loops. Such figures can show stability regions and point out potential instability problems than can be caused by either placing the controllers on automatic or by switching some of them to manual. The figures also

can be used as an indication of interaction in a system, as any alteration in the stability limits of a controller as a result of switching on or off another controller is seen as an indicator of interaction in the system.
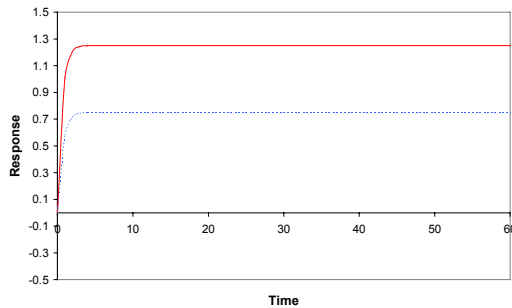
(a) Response to a unit step change in x_1sp

(loop x_1-u_2 only on automatic)
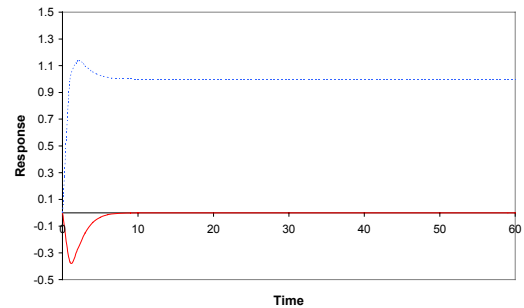
(b) Response to a unit step change in x_2sp

(loop x_2-u_1 only on automatic)
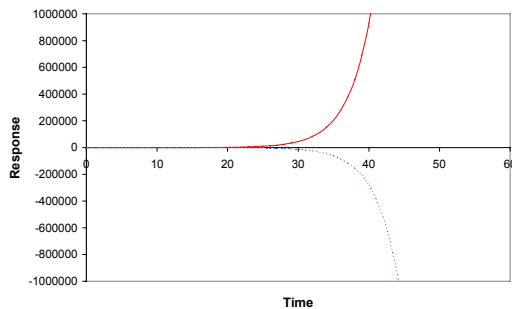
(c) Response to a unit step change in x_1sp

(both loops on automatic)
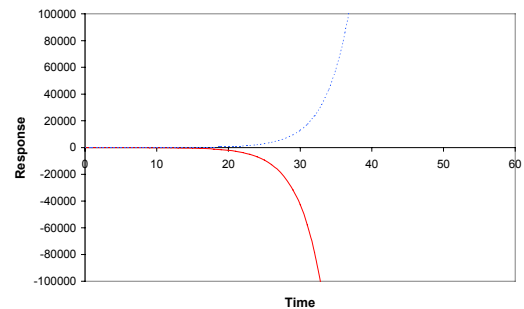
(d) Response to a unit step change in x_2sp

(both loops on automatic)

——— x_1 - - - - x_2

Figure 7.7: Responses of x_1 and x_2 to unit changes in their set points (x_1-u_2 & x_2-u_1 pairings). Interaction between the loops shows instability so long as both loops are closed

7.1.2. Application to the Refrigeration Case Study

An attempt was made to apply the analysis method described in the previous section to the two-stage refrigeration system, utilising the symbolic toolbox in MATLAB to determine the characteristic equation and the transfer functions between the variables. However, graphs similar to Figures 7.3 and 7.6 cannot be produced directly because with five controllers there is a need for five-dimensional graphs, thus limiting the

analysis to determine the controller gains in a maximum of three closed loops at a time (with 3 dimensional plots). The other two control loops would have been fixed settings for a given plot.

For the refrigeration system, Wilson and Jones (1994) showed that the two liquid level control loops interact. Consequently, an attempt to produce graphs similar to Figures 7.3 and 7.6 for the stability regions between the two level control loops was made. The other three control loops had fixed tuning (see Table 5.3). The results of the analysis were extremely complicated, and difficult to plot. To illustrate the degree of complexity, the resulting characteristic equation is

$$
\begin{aligned}
400\,[&5.553e32s^{12} \\
+&(2.14e34 + 4.03e32\,k_1 + 6.78e32\,k_2)s^{11} \\
+&(3.33e34 + 1.52e32\,k_1 + 2.43e32\,k_2 + 4.93e30\,k_1k_2)\,s^{10} \\
+&(2.65e32 + 2.30e32\,k_1 + 3.48e31\,k_2 + 1.78e30\,k_1k_2)\,s^{9} \\
+&(1.13e31 + 1.77e30\,k_1 + 2.55e30\,k_2 + 2.59e29\,k_1k_2)\,s^{8} \\
+&(2.47e29 + 7.28e28\,k_1 + 1.00e29\,k_2 + 1.89e29\,k_1k_2)\,s^{7} \\
+&(2.31e27 + 1.53e27\,k_1 + 2.03e27\,k_2 + 7.40e27\,k_1k_2)\,s^{6} \\
+&(4.45e24 + 1.39e25\,k_1 + 1.78e25\,k_2 + 1.48e25\,k_1k_2)\,s^{5} \\
+&(2.29e21 + 2.65e22\,k_1 + 3.43e22\,k_2 + 1.27e23\,k_1k_2)\,s^{4} \\
-&(1.53e17 + 1.37e19\,k_1 + 1.83e19\,k_2 + 2.43e20\,k_1k_2)\,s^{3} \\
+&(1.73e12 - 8.55e14\,k_1 - 5.58e14\,k_2 + 1.30e17\,k_1k_2)\,s^{2} \\
+&(2.13e7 + 1.05e10\,k_1 - 3.08e9\,k_2 - 4.20e12\,k_1k_2)\,s \\
+&(4.70e1 + 5.53e4\,k_1 - 5.18e3\,k_2 - 1.82e7\,k_1k_2)] = 0
\end{aligned}
\tag{7.16}
$$

Attempts to construct the Routhian Array for the two control loops resulted in impractical and cumbersome solutions.

Analysis of the 2 × 2 simple example and the refrigeration system illustrate that the closed loop approach discussed is only successful for simple low order systems as its application to high order systems is cumbersome and makes large computational demands.

7.2. INSIGHTS INTO OPEN LOOP BEHAVIOUR USING GRAPH THEORY

All the interaction measures investigated in Chapter 6 based their analysis on the system transfer function matrix **G**. Although this matrix gives the relationship between

the inputs and outputs, it fails to identify the underlying loops between the inputs and the outputs themselves. Also, the closed loop approach discussed in the Section 7.1 failed in high order systems.

In designing any control system, only a few measured variables are usually considered in the analysis. The number of these variables is in general considerably less than that of the state variables. Thus, it becomes clear that analysing the Jacobian matrix **A** is not the solution that identifies underlying loops for the following reasons:

1. The analysis cannot identify directly the interaction occurring between the measurements as it analyses only the state variables through matrix **A**.

2. If the same system is modelled in terms of different state variables, different results can be obtained. Hence the choice of state variables is introduced as an additional factor to be considered in the analysis, and this is undesirable.

Thus it makes sense to try to investigate the possibility of identifying interactions using the full state space model matrices in a way that can reveal the underlying relationships between the inputs and outputs. Such a solution will not only analyse directly these relationships, but will also cut significantly the amount of calculation needed and will not be affected by the choice of state variables used in formulating the model. In the next section, a method is described which makes use of this idea.

7.2.1. Developing the Input / Output Interaction Array (IOIA)

A new steady state interaction measure, the Input / Output Interaction Array IOIA, is proposed here, taking as its starting point the idea of Johnston (1990) of dividing the steady state gain of a pairing into "Direct Effect" and "Indirect Effect". Here the Direct Effect is the non-interactive effect between u_i and y_i, whereas all other effects between u_i and y_i are denoted Indirect Effect. The steady state gain is the sum of the Direct Effect and the Indirect Effect.

To achieve this, the state space model described in Equations 2.1 and 2.2 is transformed into a form that defines the relationship between the measurements and the manipulated variables. The derivation of the IOIA is explained below.

From the state space model, the measurements are defined as

$$\mathbf{y} = \mathbf{C}\,\mathbf{x} + \mathbf{D}\,\mathbf{u} \qquad\qquad (2.2)$$

Taking the derivative of Equation 2.2 with respect to time

$$\frac{d\mathbf{y}}{dt} = \mathbf{C}\,\frac{d\mathbf{x}}{dt} + \mathbf{D}\,\frac{d\mathbf{u}}{dt} \qquad\qquad (7.17)$$

From the standard state space equation

$$\frac{d\mathbf{x}}{dt} = \mathbf{A}\,\mathbf{x} + \mathbf{B}\,\mathbf{u} \qquad\qquad (2.1)$$

Substituting Equation 2.1 in Equation 7.17 leads

$$\frac{d\mathbf{y}}{dt} = \mathbf{C}\,\mathbf{A}\,\mathbf{x} + \mathbf{C}\,\mathbf{B}\,\mathbf{u} + \mathbf{D}\,\frac{d\mathbf{u}}{dt} \qquad\qquad (7.18)$$

Rearranging Equation 2.2 gives

$$\mathbf{x} = \mathbf{C}^{-1}\,(\mathbf{y} - \mathbf{D}\,\mathbf{u}) \qquad\qquad (7.19)$$

Note that the psuedo-inverse as defined in MATLAB is used to evaluate $\mathbf{C}^{-1}$ when $\mathbf{C}$ is not a square matrix. The psuedo-invesre has been used by Chang and Yu (1989) in evaluating the non-square RGA.

Substituting in 7.18 gives

$$\frac{d\mathbf{y}}{dt} = \mathbf{C}\,\mathbf{A}\,(\mathbf{C}^{-1}\,\mathbf{y} - \mathbf{C}^{-1}\,\mathbf{D}\,\mathbf{u}) + \mathbf{C}\,\mathbf{B}\,\mathbf{u} + \mathbf{D}\,\frac{d\mathbf{u}}{dt} \qquad\qquad (7.20)$$

Expanding the brackets and collecting terms

$$\frac{d\mathbf{y}}{dt} = \mathbf{C}\,\mathbf{A}\,\mathbf{C}^{-1}\,\mathbf{y} + (\mathbf{C}\,\mathbf{B} - \mathbf{C}\,\mathbf{A}\,\mathbf{C}^{-1}\,\mathbf{D})\,\mathbf{u} + \mathbf{D}\,\frac{d\mathbf{u}}{dt} \qquad\qquad (7.21)$$

So the matrix **E** can be defined as

$$\mathbf{E} = \mathbf{C} \, \mathbf{A} \, \mathbf{C}^{-1} \tag{7.22}$$

And the matrix **F** can be defined as

$$\mathbf{F} = \mathbf{C} \, \mathbf{B} - \mathbf{C} \, \mathbf{A} \, \mathbf{C}^{-1} \, \mathbf{D} = \mathbf{C} \, \mathbf{B} - \mathbf{E} \, \mathbf{D} \tag{7.23}$$

At steady state, $\dfrac{d\mathbf{y}}{dt} = \dfrac{d\mathbf{u}}{dt} = 0$. Hence Equation 7.21 reduces to

$$\underline{\mathbf{0}} = \mathbf{E} \, \mathbf{y} + \mathbf{F} \, \mathbf{u} \tag{7.24}$$

The IOIA uses the transformed system matrices (i.e. matrices **E** and **F** defined in Equations 7.22 and 7.23) to determine the ratio of the Direct Effect to the Indirect Effect between variables in **u** and **y** at steady state.

At steady state, Equation 7.24 is rearranged into the form

$$
\begin{aligned}
y_1 &= (-1/e_{11}) * [(e_{12}\, y_2 + e_{13}\, y_3 + \ldots.) + (f_{11}\, u_1 + f_{12}\, u_2 + \ldots.)] \\
&\ldots \\
y_n &= (-1/e_{nn}) * [(e_{n1}\, y_1 + e_{n2}\, y_2 + \ldots.) + (f_{n1}\, u_1 + f_{n2}\, u_2 + \ldots.)]
\end{aligned}
\tag{7.25}
$$

The Direct Effect between y_i and u_j is denoted as **De**. The ij^{th} element of **De** is expressed as

$$\mathbf{De} = \{de_{ij}\} = \left\{ \frac{-f_{ij}}{e_{ii}} \right\} \tag{7.26}$$

And the Indirect Effect, denoted as **Ie**, is all the rest, and is calculated as

$$\mathbf{Ie} = \{ie_{ij}\} = \{ g_{ij}(0) - de_{ij}\} \tag{7.27}$$

Elements in the IOIA are defined as the ratio of the Direct Effect to the Indirect Effect.

For the y_i-u_j pairing, this is expressed as:

$$\mathbf{IOIA} = \{ioia_{ij}\} = \left\{\frac{de_{ij}}{ie_{ij}}\right\} \qquad (7.28)$$

A MATLAB program to perform these calculations is presented in Appendix C.

If the pairing y_i-u_j does not suffer interaction from other system pairings then the Indirect Effect is zero and the ij^{th} IOIA element will be infinity. The best pairings are those which have the largest (absolute value) IOIA elements. IOIA elements of unity indicate equal Direct and Indirect Effects, and elements below 1 indicate that the Indirect Effect is larger than the Direct Effect in the ij^{th} pairing. Negative values indicate that the Direct and Indirect Effect are in opposite directions.

It should be noted that elements in the IOIA are scaling independent. Also, like the RGA this array is not intended to give a quantitative measure of the interaction in sets of pairings but only a pairing guidance.

7.2.2. IOIA Applied to the 2 × 2 Simple System

The application of the IOIA was first performed on the 2 × 2 simple example defined in Equation 7.1.

Starting from the system matrices **A**, **B**, **C**, and **D**, and using Equations 7.22 and 7.23, the matrices **E** and **F** are calculated as:

$$\mathbf{E} = \begin{bmatrix} -1 & 1 \\ 1 & -2 \end{bmatrix} \qquad (7.29)$$

and

$$\mathbf{F} = \begin{bmatrix} 2 & -1 \\ 1 & 2 \end{bmatrix} \qquad (7.30)$$

Note that in this example, the measured variables are the state variables, hence the matrix **C** is the identity matrix and therefore matrices **A** and **E** are identical.

Applying Equation 7.26, the Direct Effect matrix **De** is then calculated as

$$\mathbf{De} = \begin{bmatrix} 2 & -1 \\ 0.5 & 1 \end{bmatrix} \tag{7.31}$$

Remembering that the steady state gain matrix **G**(0) is

$$\mathbf{G}(0) = \begin{bmatrix} 5 & 0 \\ 3 & 1 \end{bmatrix} \tag{7.2}$$

The IOIA is then calculated as

$$\mathbf{IOIA} = \begin{bmatrix} 0.667 & -1 \\ 0.2 & \infty \end{bmatrix} \tag{7.32}$$

The best pairing indicated by the IOIA is x_2-u_2 associated with the infinite element. Consequently the only other pairing possible is x_1-u_1 which is associated with an IOIA element of 0.667. This relatively small IOIA value, and the relatively large IOIA element (-1) associated with x_1-u_2 suggest that substantial interaction will occur in the system. ACSL simulation results for this case are shown in Figure 7.8. Here, PI controllers are used on both loops. The controller gain factors are both 1, and the integral times are 2.618. Figures 7.8a and 7.8b show the existence of interaction as both x_1 and x_2 react to a disturbance on the opposite set point while their loops are on manual.

In Figures 7.8c and 7.8d, the significance of the IOIA elements can be seen, as interaction between the two control loops is evident as variables respond as a result to a step change in either set point. This behaviour was not predicted by the RGA which suggested that no interaction occurs in this case.
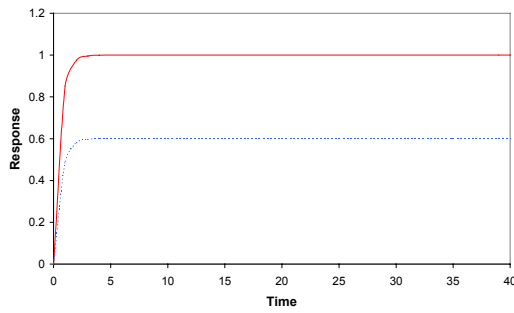
(a) Response to a unit step change in x_1sp
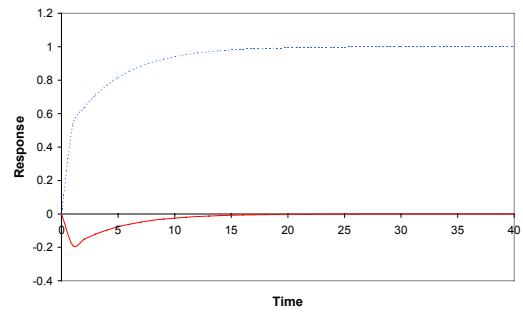
(loop x_1-u_1 only on automatic)

(b) Response to a unit step change in x_2sp

(loop x_2-u_2 only on automatic)
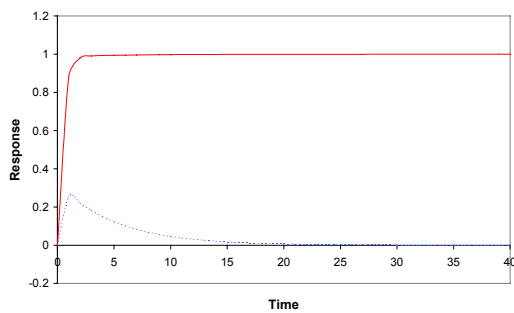
(c) Response to a unit step change in x_1sp

(both loops on automatic)
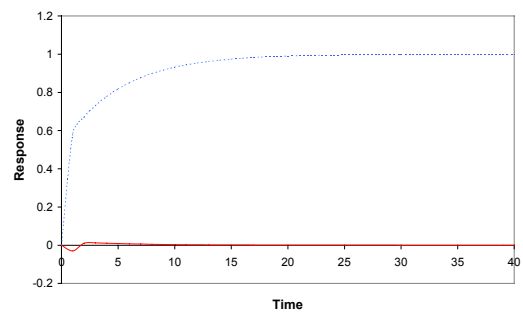
(d) Response to a unit step change in x_2sp

(both loops on automatic)

—— x_1 - - - - x_2

Figure 7.8: Responses of x_1 and x_2 to unit changes in their set points (x_1-u_1 & x_2-u_2 pairings) illustrating interaction in the system

7.2.3. IOIA Applied to the Refrigeration Case Study

The IOIA analysis was applied to the two-stage refrigeration system for Cases 1 to 5 (defined in Table 6.1). The resulting IOIA matrices are shown in Table 7.1.

The application of the IOIA pairing guidance on Case 1 is explained in detail. The first pairing to be chosen is the one associated with the largest element (absolute value) in the IOIA. Examining the IOIA matrix for Case 1 shows that this element is 176.7 which corresponds to the pairing P2-XV1. Fixing this pairing removes the row associated with P2 and the column associated with XV1 from further pairing consideration. The next largest element in the remaining array is 12.3 which corresponds to the pairing P1-N, hence fixing it removes the associated row and column leaving a 3 × 3 array. The next largest remaining element fixes the pairing L1-

XV2 (4.5), then P3-FCP3 (3.8). Consequently, the last pairing is fixed by default as L2-XV3 (0.42), this is associated with a small IOIA element suggesting high interaction.

Table 7.1: IOIA results for the refrigeration system case study *

Case	IOIA				
1 Base-Con	XV2	XV3	N	XV1	FCP3
L1	**-4.533**	0	-1.652	-0.688	0
L2	-1.436	**-0.420**	-0.098	-0.924	-0.009
P1	-0.642	0	**-12.344**	-0.887	0
P2	0.082	0.161	0.084	**176.730**	0.004
P3	0	-0.130	-2.056	-1.287	**3.803**
2 Base-Dir	XV2	XV3	N	XV1	FCP3
L1	**1.004**	0	94.335	-0.463	0
L2	-1.436	**-0.420**	-0.098	-0.924	-0.009
TP1o	-0.130	0	**-1.082**	-6.303	0
P2	0.082	0.161	0.084	**176.730**	0.004
P3	0	-0.130	-2.056	-1.287	**3.803**
3 Base-Cas	XV2	XV3	P1	XV1	FCP3
L1	**1.004**	0	-7.836	-0.463	0
L2	-1.436	**-0.420**	0.922	-0.924	-0.009
TP1o	-0.130	0	**-1.079**	-6.303	0
P2	0.082	0.161	-0.310	**176.730**	0.004
P3	0	-0.130	-2.037	-1.287	**3.803**
4 L1/L3-Cas	XV2	XV3	P1	XV1	FCP3
L1	**0.145**	0	0.409	-0.179	0
L3	0.000	**0.683**	0.469	4.354	-0.311
TP1o	-0.130	0	**-1.079**	-6.308	0
P2	0.082	0.161	-0.310	**180.450**	0.004
P3	0	-0.130	-2.037	-1.287	**3.799**
5 L2/L3-Cas	XV2	XV3	P1	XV1	FCP3
L2	**-1.490**	-0.401	0.797	-0.918	-0.008
L3	0.000	**-1.667**	-2.037	-1.250	-0.735
TP1o	-0.130	0	**-1.079**	-6.301	0
P2	0.082	0.161	-0.310	**176.790**	0.004
P3	0	-0.130	-2.037	-1.287	**3.802**

* Bold values indicate recommended IOIA pairings

A closer look at this set of pairings suggests that strong interaction will affect the L2-XV3 loop resulting from the relatively large IOIA elements in L2 row associated with XV2 (1.4) and XV1 (0.9), which means significant interaction between L2 and L1 and L2 and P2 loops.

This pairing suggested by the IOIA for Case 1 agrees with the performance results reported in Section 5.5, where the system performance was acceptable based on the ISE of TP1o. The interaction between the two liquid level loops shown by the IOIA agrees also with Wilson and Jones (1994) who identified its existence using root-locus plots.

Applying the IOIA to Case 2 fixes the first pairing as P2-XV1 (176.7). Following the same procedure already explained, the next pairings suggested are L1-N (94.3), then P3-FCP3 (3.8), then L2-XV2 (1.4), then TP1o-XV3 (0). However, the last pairing cannot be accepted as it is associated with an IOIA element of zero which indicates no Direct Effect from XV3 on TP1o, therefore the pairing procedure must be repeated by going back a step to the last remaining 2×2 array and pairing on the second largest element of the IOIA. This results in the pairings L2-XV3 (0.42) and TP1o-XV2 (0.13), where the latter pairing is associated with a small (0.13) IOIA element and hence is relatively unacceptable. Going a step further back to the 3×3 array stage results in two pairings P3-FCP3 (3.8) and TP1o-XV3 (0). Consequently the procedure is repeated from the 4×4 array stage, this time fixing P3-FCP3 (3.8) as the second pairing in the system. Following the same procedure through repeats the initial pairing which was already rejected. Hence, as the 3×3 stage, pairing moves to the second largest element and the procedure is repeated. The detailed application of the procedure is explained in Table 7.2. The final three pairings fixed are: TP1o-N (1.08), then L1-XV2 (1), then L2-XV3 (0.42). This is an acceptable result as it maximises the smallest IOIA element in the set of pairings.

Table 7.2: Application of the IOIA pairing procedure

	XV2	XV3	N	XV1	FCP3	
L1	1.004	0	94.335	-0.463	0	1. Fix the pairing P2-XV1 and remove its associated row and column
L2	-1.436	-0.42	-0.098	-0.924	-0.009	
TP1o	-0.13	0	-1.082	-6.303	0	
P2	0.082	0.161	0.084	**176.73**	0.004	
P3	0	-0.13	-2.056	-1.287	3.803	

	XV2	XV3	N	FCP3	
L1	1.004	0	**94.335**	0	2. Fix the pairing L1-N and remove its associated row and column
L2	-1.436	-0.42	-0.098	-0.009	
TP1o	-0.13	0	-1.082	0	
P3	0	-0.13	-2.056	3.803	

Table 7.2 (cont.): Application of the IOIA pairing procedure

	XV2	XV3	FCP3
L2	-1.436	-0.42	-0.009
TP1o	-0.13	0	0
P3	0	-0.13	**3.803**

3. Fix the pairing P3-FCP3 and remove its associated row and column

	XV2	XV3
L2	**-1.436**	-0.42
TP1o	-0.13	0

4. Fix the pairing L2-XV2 and remove its associated row and column

	XV3
TP1o	0

5. Remaining pairing by default is TP1o-XV3

Pairing of TP1o-XV3 is rejected as it is associated with an IOIA element of 0. Hence go back a step and re-start from the 2 x 2 matrix in Step 4

	XV2	XV3
L2	-1.436	**-0.42**
TP1o	-0.13	0

6. Fix the pairing L2-XV3 and remove its associated row and column

	XV2
TP1o	-0.13

7. Remaining pairing by default is TP1o-XV2

Pairing of TP1o-XV3 is rejected as it is associated with an IOIA of 0.13. Hence go back a step and re-start from the 3 x 3 matrix in Step 3

	XV2	XV3	FCP3
L2	**-1.436**	-0.42	-0.009
TP1o	-0.13	0	0
P3	0	-0.13	3.803

8. Fix the pairing L2-XV2 and remove its associated row and column

	XV3	FCP3
TP1o	0	0
P3	-0.13	3.803

Either choice of pairing TP1o in the above matrix will result in a pairing associated with a zero IOIA, and consequently rejected. Hence go back a step and re-start from the 4 x 4 matrix in Step 2

	XV2	XV3	N	FCP3
L1	1.004	0	94.335	0
L2	-1.436	-0.42	-0.098	-0.009
TP1o	-0.13	0	-1.082	0
P3	0	-0.13	-2.056	**3.803**

9. Fix the pairing P3-FCP3 and remove its associated row and column

	XV2	XV3	N
L1	1.004	0	**94.335**
L2	-1.436	-0.42	-0.098
TP1o	-0.13	0	-1.082

10. Fix the pairing L1-N and remove its associated row and column

contd..../

Table 7.2 (cont.): Application of the IOIA pairing procedure

	XV2	XV3
L2	-1.436	-0.42
TP1o	-0.13	0

The above matrix is a repetition of Step 4 which was rejected. Hence go back a step to the 3 x 3 matrix in Step 10

	XV2	XV3	N	
L1	1.004	0	94.335	11. Fix the pairing L2-XV2
L2	**-1.436**	-0.42	-0.098	and remove its associated
TP1o	-0.13	0	-1.082	row and column

	XV3	N
L1	0	94.335
TP1o	0	-1.082

Either choice of pairing in the above matrix will result in a pairing associated with a zero IOIA, and consequently rejected. Hence go back a step and re-start from the 3 x 3 matrix in Step 11

	XV2	XV3	N	
L1	1.004	0	94.335	12. Fix the pairing TP1o-N
L2	-1.436	-0.42	-0.098	and remove its associated
TP1o	-0.13	0	**-1.082**	row and column

	XV2	XV3	
L1	1.004	0	13. Fix the pairing L2-XV2
L2	**-1.436**	-0.42	and remove its associated
			row and column

	XV3	
L1	0	14. Remaining pairing by
		default is L1-XV3

Pairing of L1-XV3 is rejected as it is associated with an IOIA element of 0. Hence go back a step and re-start from the 2 x 2 matrix in Step 13

	XV2	XV3	
L1	**1.004**	0	15. Fix the pairing L1-XV2
L2	-1.436	-0.42	and remove its associated
			row and column

	XV3	
L2	-0.42	16. Remaining pairing by
		default is L2-XV3

Pairing is acceptable as it maximises the smallest IOIA element in the set of selected loops

The pairings determined for the remaining three cases in Table 7.1 were made following the same procedure.

The best pairings resulting from the IOIA analysis for Cases 2-5 agree with the heuristics pairings results reported in Section 5.5.

Comparing results of using the IOIA with the RGA results (see Table 6.4) shows that:

- Both methods recommend the same set of pairings for Case 1.

- The pairings recommended by the RGA for Cases 2 and 3 suggested pairing TP1o with XV2 and L1 with N (or P1 in the cascade temperature case). As shown in Section 5.5, the system performance was poor with very high ISE of TP1o, though the level controller performance was acceptable. This behaviour can be explained looking at the IOIA as the L1-N (or P1) loop corresponds to a very large IOIA element hence the good performance, and the TP1o-XV2 loop corresponds to an IOIA element of only 0.13 hence the bad performance.

- The pairings recommended by the RGA for Cases 4 and 5 failed, whereas the IOIA pairings agree with the results of Section 5.5.

7.2.4. The IOIA Applied to a Coal Gasifier

As a further example of applying the IOIA analysis approach, it is now applied to a detailed non-linear model for a coal gasifier. This model was developed and validated by GEC Alsthom. A linearised version of their ACSL model was made available to universities who participated in the MEC Benchmark Challenge, in which alternative solutions for controlling the system were called for (Dixon, 1997; Dixon *et al.*, 1998). The gasifier itself can be considered as a reactor where coal is gasified with air and steam. Pulverised coal and limestone, which is required to capture sulphur, are conveyed by pressurised air and steam, and spouted into the gasifier. The air and steam not only fluidise the solids in the gasifier, but also react with the carbon and volatiles from the coal, producing a low calorific value fuel gas. The remaining char (ash from coal, limestone and unreacted carbon) is removed as bed material from the base of the gasifier or elutriated as fines with the product gas. The fuel gas is then cleaned and fed to a gas turbine.

The control objective set was to design a control system for the linearised model of the gasifier at its 100% load operating point. In addition, the design required that control

schemes also be evaluated on models representing the 50% and 0% load cases to investigate robustness.

The gasifier is a non-linear, truly multivariable system, having five inputs (coal, limestone, air, steam and char extraction) and four outputs (pressure, temperature, bed mass and gas quality) with a high degree of cross coupling between them.

The manipulated inputs are: char extraction flow; air mass flow; coal flow; steam mass flow and limestone mass flow. The limestone absorbs sulphur in the coal so its flowrate should be set to a fixed ratio of the coal flowrate - nominally this should be to 1:10 limestone to coal. This leaves effectively 4 degrees of freedom for the control design.

The outputs are: fuel gas calorific value; bed mass; fuel gas pressure and fuel gas temperature. The set disturbance for the control systems is a step in the sink pressure, which is the gas turbine inlet pressure which would vary according to the position of the gas turbine fuel valve.

A important feature of the problem is the tight constraints on both the limits and rates of change of the manipulated variables.

A valid control design that complies with most of the system requirement is shown in Figure 7.10, and is described by Asmar *et al.* (1998b), and is presented more fully in Appendix D.

The IOIA analysis was applied to the gasifier model to investigate interaction in controlling the gasifier system. The IOIA for the gasifier 100% load case is shown in Table 7.3.

Table 7.3: IOIA for the coal gasifier at 100% load

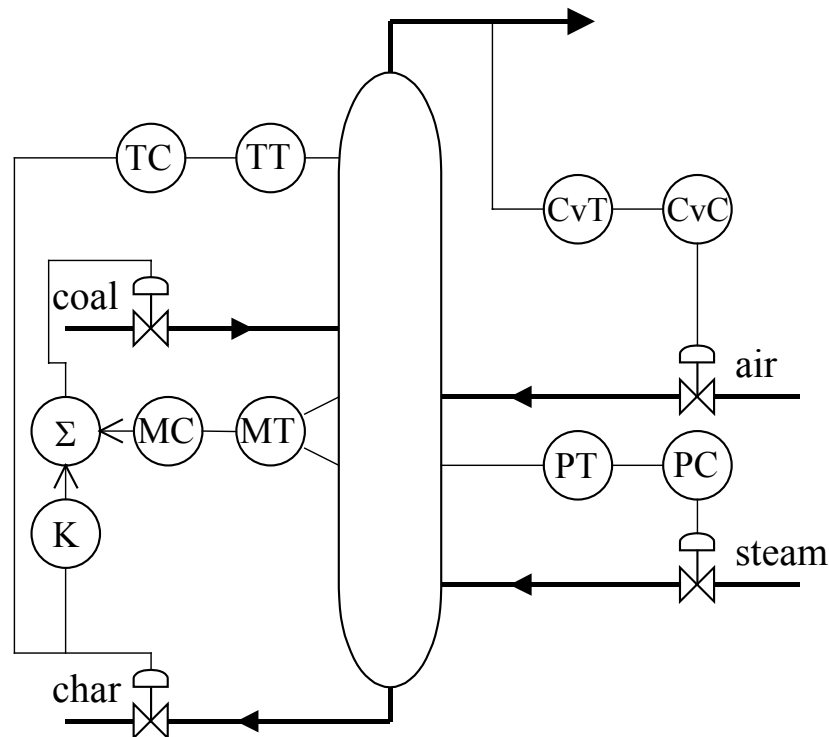|	Char	Air	Coal	Steam
C.V.	-4.87E-03	-1.37	**-1.65**	-1.45
Mass	**-1.47E-17**	2.85E-25	0	0
Pressure	7.16E-04	**-3.57**	-1.34	1.53
Temperature	-6.78E-06	6.05E-03	3.92E-04	**1.14E-03**

Figure 7.9: Control scheme of the gasifier

The pairing suggested by the IOIA is to pair P-Air, then CV-Coal, then T-Steam, then Mass-Char. This pairing was also recommended by the RGA. It was applied to the gasifier system and was simulated as Scheme 1 in Appendix D. Although the control system was successful, the strict rate constraints imposed on inputs and outputs made it unacceptable as a valid answer.

Repeating the IOIA pairing procedure starting from the second largest element results in the following pairing: CV-Coal, P-Steam, T-Air, and Mass-Char. This pairing was also applied to the gasifier system and was simulated as Scheme 2 in Appendix D. Although the control system was successful, the strict rate constraints imposed on inputs and outputs made it again unacceptable as a valid answer.

However, the IOIA result corresponds with the acceptable performance obtained from the pairing shown in Figure 7.9. It can be explained easily, as it uses, particularly the large IOIA elements associated with the pairing CV-Air and P-Steam. The IOIA element associated with the Mass-Coal pairing is zero, thus explaining the slow drift observed in the mass response in Scheme 3, and justifies necessity of the extra link between the mass and the char in Scheme 4.

7.2.5. Discussion

The three examples above demonstrate that the IOIA can successfully identify interactive effects in control systems. They also show that it works in situations where the RGA failed. The measure can be used to assess interaction in the system at an early stage, and thus allow for the inevitable interactive effects by adapting the design at that stage.

The IOIA is based on a full state space model rather than the system transfer function matrix. It requires the availability of the full state space model matrices (**A**, **B**, **C** and **D**). Until recently, this was a problem, however, the rapid development in computer software (e.g. ACSL) make it easy to obtain linearised models numerically from their non-linear form.

In comparison with a related approach made by Johnston (1990), the closed loop SIA, the IOIA can provide an assessment for systems of any order whereas the method proposed by Johnston is only practical to low order cases as it requires the identification of all loops within the system in order to apply Mason's Rule. His calculation also requires the evaluation of the manipulated variables changes to keep the controlled variables (except the variable in the pairing investigated) unchanged.

In the case of the refrigeration system, which is of prime interest in this thesis, applying the IOIA analysis shows that the simulation results of heuristics pairings which were used in Chapter 5 validate the resulting IOIA pairings.